Periodica Polytechnica
Mechanical Engineering

Frequency and Phase Characteristics of the Edge Tone Part I.

58(1), pp. 55-67, 2014
DOI:10.3311/PPme.7028

István Vaik, *Roxána* Varga, *György* Paál

RESEARCH ARTICLE

RECEIVED 3 SEPTEMBER 2013

Abstract

This paper is the first half of a two-part publication. In these papers the well-known low Mach number edge tone configuration is investigated which is one of the canonical self-sustained flow configurations leading to simple aeroacoustic flow phenomena. The configuration consist of a planar free jet that impinges on a wedge shaped object. Under certain circumstances the jet starts to oscillate more or less periodically thereby creating an oscillating force on the wedge that acts as a dipole sound source.

This first part contains a detailed literature overview and the qualitative discussion of the authors' results of a detailed parametric study. The formulae in the literature describing the dependence of the frequency on exit velocity and nozzle-wedge distance show a broad scatter, although similar in form. In this paper a systematic and thorough study is made by experimental and numerical means and remarkable agreement is found.

Keywords

Edge tone

István Vaik
Roxána Varga
Department of Hydrodynamic Systems,
Budapest University of Technology and Economics
György Paál
Department of Hydrodynamic Systems,
Budapest University of Technology and Economics
e-mail: paal@hds.bme.hu

1 Introduction

1.1 What is the edge tone?

The edge tone is one of the simplest aero-acoustic flow configurations. It consists of a planar free jet that impinges on a wedge-shaped object (traditionally called the edge). The main parameters of an edge tone configuration are the mean exit velocity of the jet (u), the width of the jet (δ) and the nozzle-to-wedge distance (h) (Figure 1). Secondary parameters may also influence the flow, such as the velocity profile of the jet (top hat and parabolic profiles are the most common ones), the offset of the wedge from the jet center line, the shape of the nozzle or the angle of the wedge. Despite its geometric simplicity, the edge tone displays a remarkably complex behaviour. Under certain circumstances a self-sustained oscillation evolves with a stable oscillation frequency. The oscillating jet creates an oscillating force on the wedge, that generates a dipole sound source, and under certain circumstances creates an audible tone.

The oscillating jet can take different shapes, these are called the stages of the edge tone. Their ordinal number corresponds roughly to the number of half waves between the nozzle and the wedge. Figure 1 shows snapshots of the flow fields of first stage edge tone flows. Figure 1(a) is from a computational fluid dynamics (CFD) simulation and Figure 1(b) is from the experimental investigation of the flow field. In both cases the flow is visualised by smoke introduced in the central part of the nozzle.

Figure 2(a) shows what happens with the oscillation frequency when the velocity is varied in a fixed geometrical configuration (at constant δ and h values). At low velocities the wedge cuts the jet in half and a steady flow is formed. Increasing the velocity above a certain threshold velocity – whose value depends on the geometrical configuration – the first stage of the edge tone sets in (position A). With increasing jet velocity the second stage comes into being with a sudden jump in the frequency to a higher value (position B). Usually the first stage still coexists with the new, second stage, thus a multi-stage operation mode can be observed although the second stage can be present purely as well. At higher velocities the third stage of the edge tone is formed (position C) – again with a sudden jump in the frequency to a higher value –

either with some of the lower stages coexisting, or purely. As the jet velocity is increased, even higher stages may evolve, with a jump in the frequency to a higher value at the onset of each new stage. Similar behaviour can be observed when the velocity of the jet is decreased. The frequency of the oscillation decreases, and at a point the highest stage disappears (at positions C' and B' the third and the second stage disappears, respectively) with a sudden drop in the frequency and at last at small jet speeds the first stage of the edge tone disappears and a steady flow is formed (position A'). It can be that the velocity value at the point where a stage disappears during the decrease of the jet velocity (position C', B' or A') differs from the velocity value at the point where this stage first appeared when the velocity was increased (position C, B or A), so hysteresis may occur.

On the other hand, when the nozzle-to-wedge distance is varied while the velocity of the jet is kept constant (Figure 2(b)), the following can be observed. At low distances no oscillation occurs. Increasing the distance, at a certain lower limiting value the first stage of the edge tone forms (position A). With further increases in the distance, the frequency of the oscillation decreases. At a point the second stage sets in with a sudden jump in the frequency to a higher value (position B). As the distance is further increased, the frequency again decreases until the next stage forms with the sudden jump in the frequency again to a higher value (position C). Now, if the nozzle-to-wedge-distance is decreased from a higher value, then the frequency of oscillation increases until a certain position where the jet jumps back to a lower stage where the frequency is also lower (position C' and B') and at last the oscillation disappears completely (position A'). Just as in the case when the velocity is varied, hysteresis may occur; it can happen that the jump between the stages back and forth are at different positions ($A \neq A'$ or $B \neq B'$ or $C \neq C'$).

The following dimensionless numbers will be used throughout the paper:

- **Reynolds number** based on the mean exit velocity of the jet and the width of the jet will be used as the dimensionless jet velocity: $Re = u\delta/\nu$
- **Strouhal number** based on the frequency of oscillation (f), the width of the jet and the mean exit velocity of the jet will be used as the dimensionless oscillation frequency: $St = f\delta/\nu$
- ***h/δ*** will be used as the dimensionless nozzle-to-wedge distance

Because of scaling laws, two edge tone configurations with different jet velocities and geometric sizes but at the same Reynolds number and h/δ dimensionless nozzle-to-wedge distances produce oscillations with different frequencies but with the same Strouhal numbers, therefore when comparing results from different sources (theoretical and/or experimental and/or numerical) comparison of the Strouhal numbers at same Reynolds numbers and at same h/δ values will be carried out.

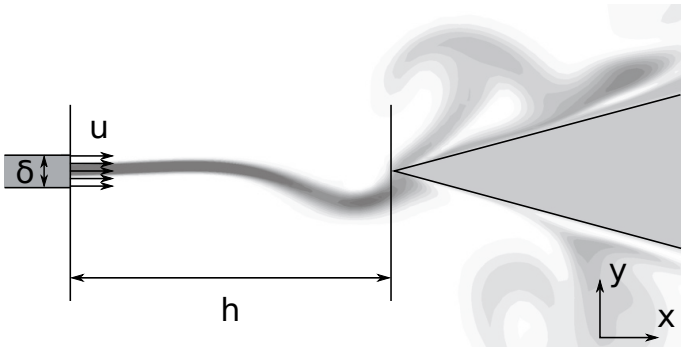

(a) from a CFD simulation using virtual smoke with the main parameters of the edge tone configuration (δ – width of the slit on the nozzle; h – nozzle-to-wedge distance; u – mean exit velocity of the jet)

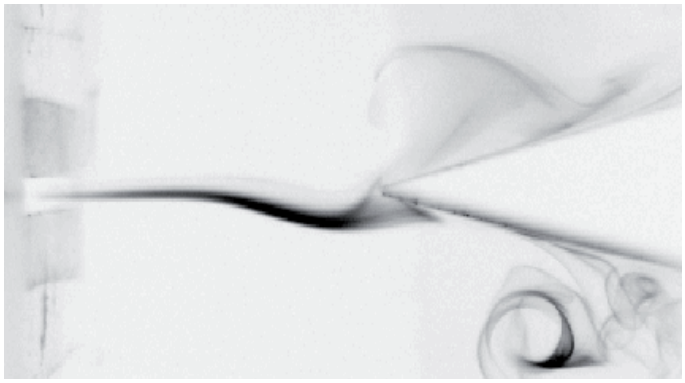

(b) from an experiment, using real smoke;

Fig. 1. Snapshots of a first stage edge tone flow

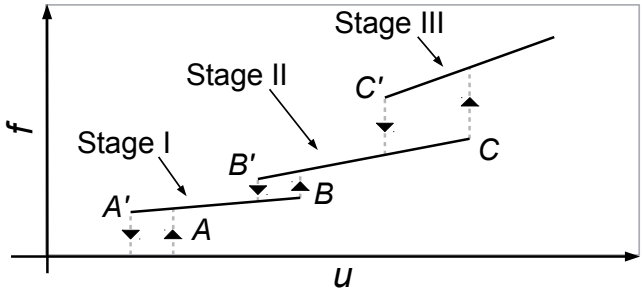

(a)

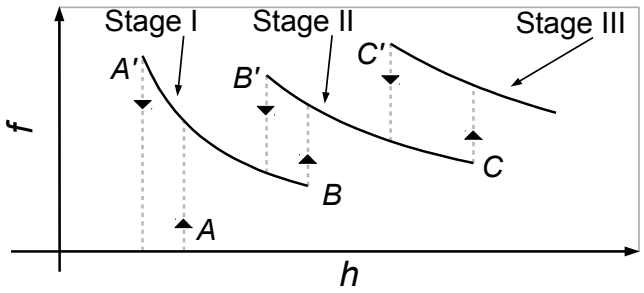

(b)

Fig. 2. Characteristics of frequency variation as a function of (a) jet velocity and (b) nozzle-to-wedge distance

1.2 Literature overview

Brown [5,6] gave a detailed overview on the early research on the edge tone phenomenon from the first 80 years after it was first noted by Sondhaus in 1854. Several researchers tried to explain the mechanism of the edge tone production theoretically, others made extensive experimental investigations in the field. Without being exhaustive we shall give a short introduction to the most important studies. At first, we shall review the theories (in chronological order), then the experimental and numerical studies.

1.2.1 Theories

Curle [9] published his purely hydrodynamic vortex theory, explaining the edge tone in 1953. He claimed that vortices of opposite circulation are produced at the nozzle (embryo vortex) and at the tip of the wedge (secondary vortex) at the same time. The formation of the secondary vortex takes place when the transverse velocity at the tip of the wedge is maximum; that occurs halfway between the alternating vortices below and above the wedge. Thus the relationship between the nozzle-to-wedge distance and the wavelength is: $h = (n + 1/4)\lambda$, where n denotes the ordinal number of the stage and λ the distance between two consecutive vortices on the same side of the jet. Independently of this result he deduced a semi-empirical formula for the velocity with which the vortices move (u_{conv}) in the case when $h/\delta > 10$:

$$\frac{u_{conv}}{u} = \frac{1}{2}\left(1 - \frac{\lambda}{30\delta}\right), \tag{1}$$

thus the frequency of oscillation of the n^{th} stage is:

$$f = \frac{1}{2}u\left(\frac{n+\frac{1}{4}}{h} - \frac{1}{30\delta}\right) \tag{2}$$

He suggests that n has a value such that

$$\lambda = \frac{h}{n+\frac{1}{4}}$$

is near the wavelength for which an edgeless jet is most sensitive, and after stage jumps λ gets closer to this value.

Curle also emphasises that if Savic's [24] result of

$$\frac{u_{conv}}{u} = 1.024\sqrt{\frac{\delta}{\lambda}}$$

is used instead of his semi-empirical formula (1), then the frequency of oscillation becomes:

$$f = \frac{u\delta^{\frac{1}{2}}}{h^{\frac{3}{2}}} \cdot c, \tag{3}$$

where c = 1.43; 3.46; 6.00 and 8.98 for the first four stages.

In 1954 Nyborg published his dynamic theory explaining the edge tone phenomenon [19]. His theory assumes that due to a kind of sources of "hydrodynamic" origin at the wedge transverse forces act on each particle of the jet as it travels toward the wedge. He dealt with only the centreline of the jet, and supposed that the vertical acceleration acting on any particle travelling towards the wedge depends only on two factors: its instantaneous horizontal distance from the wedge and the instantaneous jet displacement at the wedge. With his theory, Nyborg was able to describe the shape of the centreline of the jet. Although he was not able to determine the frequency of oscillation, he was able to determine the ratio of the frequencies of the different stages (1 : 2.44 : 3.86 : 5.29 for the first four stages). He also indicated that as h increases, higher modes become possible. He found the lower limit of the n^{th} stage to be $h/\delta > 2n$ but the theory is not capable to predict the position where the jet jumps from one stage to another. Since his dynamic theory only deals with the centreline of the jet it fails to predict that the frequency of oscillation depends on the width of the jet.

Powell first published his feedback loop theory in 1953 and then later, in 1961 he gave its detailed discussion [22,23]. He suggested that an infinitesimal excitation at the nozzle exit grows along the jet via an instability displacement wave. This distortion generates an oscillating force on the wedge that creates a dipole sound source, which then closes the loop by exciting the jet at the nozzle exit. Despite the feedback loop being based on the dipole sound source, he stated that the feedback loop is purely hydrodynamic, the sound radiation itself does not play an essential role in the mechanism. From this feedback loop a phase criterion can be deduced implying the oscillation frequency of the n^{th} stage to be:

$$f = \left(n + \frac{1}{4}\right)\frac{u_{conv}}{h}, \tag{4}$$

where u_{conv} is the convection velocity of the disturbances. He emphasises that the frequencies of the stages do not bear ratios of 5/4 : 9/4 : 13/4, because sinuosities of different wavelengths have different convection velocities.

For the stage jumps Powell gave the following explanation: for any given u_{conv} and h values a certain f frequency can be calculated for each of the stages from Equation (4). For low nozzle-to-wedge distances these frequencies will be well above the regime where the edge-less jet is sensitive to acoustic excitations even for the first stage, thus the edge tone phenomenon will not occur. As the nozzle-to-wedge distance is increased to a point the frequency of the first stage reaches the regime of sensitivity, and the first stage of the edge tone sets in. Further increasing the nozzle-to-wedge distance the oscillation frequency decreases and at a point it reaches the lower boundary of the sensitivity regime and the first stage disappears. At this point the frequency of the second stage is already in the sensitivity regime, thus by this point the edge jumps to the second stage.

A similar explanation can be given for the onset of the stages in the case of a fixed geometric configuration with varying jet velocity.

Powell noted that it can happen that the new stage is superimposed on the old stage, and the two stages coexist. He also noted that it is more likely than not that the jumps between the stages will be hysteretic. He experimentally showed the dipole characteristics of the edge tone sound field, and showed that the amplitude of the acoustic pressure is proportional to the third power of the jet velocity.

Holger et al. developed a vortex street theory in 1977 [10]. Their assumptions were that the wavelength of the jet disturbance, the width of the vortex street and the propagation velocity of the vortices are constant. While Curle based his vortex theory on the formation of secondary vortices at the edge, Holger et al.'s analysis does not depend on secondary vortices, and used an entirely different formula for describing the oscillation frequency. Contrary to Powell, they assumed that the vortex street is fully formed by the time it interacts with the edge. They found the frequency of oscillation to be:

$$f = 0.925\left(\frac{\delta}{h}\right)^{\frac{1}{2}} \frac{u\left(n+\alpha_n\right)^{\frac{3}{2}}}{h}, \tag{5}$$

where $\alpha = 0.4$; 0.35 and 0.5 for the first, the second and the third stages, respectively.

In 1980 Holger et al. [11] extended their theory and gave an approximation for the vertical force acting on the wedge. From this they were able to calculate the acoustic pressure at an arbitrary point in the far field with Lighthill's equation. They found that the integration length on the wedge should be chosen as 2λ, and in this case the calculated force is

$$F \approx 1.08\rho W u^2 \delta, \tag{6}$$

where ρ is the density of the fluid and W is the height of the flow. From this, the amplitude of the acoustic pressure at a distance r in the direction of maximum radiation is

$$\left|p_a\right| = \frac{fF}{2ra_0} \approx 0.5\left(\frac{\delta}{h}\right)^{\frac{3}{2}} \left(n+\alpha_n\right)^{\frac{3}{2}} \frac{\rho u^3 W}{ra_0}, \tag{7}$$

where a_0 is the speed of sound. They also noticed that the vortex pair nearest to the tip of the wedge gives the most significant part of the force, and the instantaneous force has its maximum when the distance between the tip of the wedge and the first vortex downstream of it is 0.1λ.

In 1992 Crighton [8] created a linear analytical model to predict the frequency characteristics of the edge tone oscillation. He dealt with a top hat jet impinging on a plate placed parallel to the flow in the center of the jet. He assumed inviscid flow with vortex-sheet shear layers, and solved the problem asymptotically by Wiener-Hopf methods. He found that the dimensionless oscillation frequency – $S = \omega b/u$, where $\omega = 2\pi f$ is the angular frequency and $b = \delta/2$ is the jet half-thickness – is

$$S = \left(\frac{b}{h}\right)^{\frac{3}{2}} \left[4\pi\left(n-\frac{3}{8}\right)\right]^{\frac{3}{2}}, \tag{8}$$

and the h/λ ratio is $(n - 3/8)$. He found that his Strouhal number (defined as at the beginning of the Introduction) is much larger than the values reported by Holger et al. For the relative convection velocity of the disturbance he used the

$$\frac{u_{conv}}{u} \approx 2S^{\frac{1}{3}}$$

formula, while Holger et al. used

$$\frac{u_{conv}}{u} \approx 0.645S^{\frac{1}{3}}.$$

Without essentially finding the cause of this large difference, he concludes that his formula would give a better prediction if

$$\frac{u_{conv}}{u} \approx \frac{2S^{\frac{1}{3}}}{1+\frac{4}{3}S^{\frac{1}{3}}}$$

were used but (we cite, [8] p. 386) "all such expressions would lead to the same behaviour, namely preservation of essentially the form of equation (8) but with

$$\left(4\pi\right)^{\frac{3}{2}}$$

replaced by a smaller coefficient".

In 1996 and 1998 Kwon [14,15] presented a theoretical model in which the jet-edge interaction was modelled by an array of dipoles on the edge. By assuming the jet to oscillate sinusoidally and the convection velocity of the disturbances to be constant, his model can estimate the surface pressure distribution on the wedge, and from that an array of acoustic dipoles on the wedge can be deduced. Kwon found that the peak value of the spatial pressure distribution on the wedge can be found approximately a quarter wavelength downstream of the tip of the wedge. He found that the phase criterion is:

$$\frac{h}{\lambda} + \frac{h}{\Lambda} = n - \frac{1}{4},$$

where Λ is the wavelength of the upstream propagating disturbance (the acoustic field of the dipole sources). Thus, he claims that the point of the wedge surface where the pressure has its maximum (a quarter wavelength downstream of the tip) is the position of the effective acoustical source. Kwon also found that the convection velocity of the disturbance on the jet is approximately 60% of the mean exit velocity of the jet,

and thus the Strouhal number of the oscillation can be approximated as:

$$St = \frac{h}{\delta}\frac{n-\frac{1}{4}}{1.667+Ma}, \tag{9}$$

where Ma is the Mach number of the mean jet velocity ($Ma = u/a_0$).

1.2.2 Experiments

In 1937 Brown [5,6] investigated an edge tone setup of a $\delta = 1$ mm wide, top hat jet with a wedge with an angle of 20° experimentally. He found that the whole edge tone phenomenon occurs at frequencies for which the edgeless jet is sensitive to sound and the frequency of the stages depends on the exit velocity of the jet and the nozzle-to-wedge distance through the following formula:

$$f = 0.466 \cdot j \cdot (u-40)\left(\frac{1}{h}-0.07\right), \tag{10}$$

where u and h are measured in cm/s and in cm, respectively, and $j = 1, 2.3, 3.8,$ and 5.4 for the first, the second, the third and the fourth stage, respectively. Brown claimed that the deviation between his measurement and his formula for jet velocities $u = 120 – 2000$ cm/s (that is in nondimensional values $Re = 75 – 1300$) and frequencies $f = 20 – 5000$ Hz was maximum 6%. He found the limits of h to be 0.31 cm and 6 cm, so that the nondimensional nozzle to wedge distance was between 3.1 and 60.

Brown found that for higher stages the first stage could also be coexisting, and in this case the frequency of the first stage is about 7% lower than the frequencies predicted by his formula. As the formula can have as much as 6% deviation from the measured values he concluded that this drop in the frequency practically can be neglected.

In the case of higher stages he measured the wavelength of the jet disturbance as the distance between two successive vortices on the same side of the stream (from the photographs he took of the visualised flow), while for Stage I he assumed that $\lambda = h$. With this and the measured oscillation frequency he calculated the convection velocity of the vortices as $u_{conv} = f \cdot \lambda$ that resulted in values of about 40% of the jet exit velocity ($u_{conv}/u \approx 0.4$).

Brown also investigated how sound production effects the edge tone, and concluded that in some cases acoustical excitation can control the stages of the edge tone.

In 1942 Jones [12] investigated an edge tone configuration with a 0.8 mm wide top-hat jet, at velocities up to 50 m/s, and with nozzle-to-wedge distances between 5 and 25 mm. In his experiments the wedge angle was 25°. He reported two types of edge tone. In the first type – that occurs at lower jet velocities – he found three stages, between which jumps in the oscillation frequency occur. In the second type of the edge tone – that occurs at higher jet velocities (above ≈ 37 m/s) – the jet is probably turbulent and no jumps occur if the parameters are varied but the frequency changes continuously. He found that the frequencies of the three stages of the first type edge tone oscillation and also that of the second type can be described as:

$$f = j \cdot \frac{u}{h^k}, \tag{11}$$

where u is measured in cm/s, h in mm. The values of j and k for the three stages of the first type and for the second type are: $j = 3.9, 11.8, 24$ and 6.8; $k = 1, 1.14, 1.22$ and 1.43, respectively.

In 1952 Nyborg et al. [20] made an extensive experimental research in mapping the stage boundaries in the $h – q$ plane (where q is the volumetric flow rate of the air, thus in a given geometric configuration proportional to the velocity of the jet) of small edge tones ($\delta = 0.25 – 1.02$ mm) with high frequency oscillations (f up to 200 kHz). They used parabolic jets with different widths and several (in some cases asymmetric) wedges that sometimes were placed with a transversal offset from the center of the jet.

They compared their measured frequencies to a somewhat simplified form of Brown's semi-empirical formula (equation (10)), namely:

$$f = 0.466 \cdot j \cdot u / h, \tag{12}$$

and found that, the measured values agree well with the simplified formula at $f \approx 2.5$ kHz but are slightly lower than the formula below 2.5 kHz and are a bit higher than the formula above 2.5 kHz.

They found that the regions of the stages in the $h – q$ plane can overlap, indicating that hysteresis may occur when changing the mean exit velocity of the jet or the nozzle-to-wedge distance, and the overlapping regions are independent on the wedge angle if it is less than 40°.

They also made measurements on the directivity of the sound emitted by the edge tone, and found that at $f < 10$ kHz a cosine law (dipole radiation pattern) fits their experimental results fairly well. Above 10 kHz they found a directivity pattern with double maxima that they were not able to explain.

Brackenridge and Nyborg [4,3] reported experiments on top hat underwater edge tones with three different jet widths ($\delta = 0.51$ mm, 1.02 mm and 2.04 mm) and a wedge with an angle of 28°. They found that – in the case of $\delta = 1.02$ mm – the frequencies of the stages can be described as:

$$f = 0.63 \cdot j \cdot (u-6)\left(\frac{1}{h}-0.23\right). \tag{13}$$

They noted that the value of 0.63 seems to be dependent on the jet width.

They found that at the formation of the second stage the first one remains, and the two stages coexist. They also found nonlinear interaction of the stages: sometimes frequencies equal to

the sum and the difference of the frequencies of the two stages are also present in the spectrum. They also investigated the effect when the edge has a blade attached to its tip that can vibrate at its own frequency, and they found that this vibrating blade enforces a first stage oscillation at the blade frequency even at higher jet velocities.

In 2004 Bamberger et al. [2] made an experimental and computational investigation on a parabolic edge tone configuration with an asymmetric wedge. The Reynolds number range in their investigation was approximately $Re = 100 – 900$. In their experiments they used two different nozzles (with $\delta = 0.5$ mm and 1 mm width) and nozzle-to-wedge distances between 2.2 mm and 8.7 mm. They concentrated on the first stage oscillation only, and found that the oscillation frequency in this stage is proportional to the maximum jet velocity and inversely proportional to the nozzle-to-wedge distance:

$$f = c_d \frac{u_{max}}{h}, \tag{14}$$

where – as they claim – c_d depends on the width of the nozzle. From the experiments they concluded that for the $\delta = 0.5$ mm wide nozzle $c_{0.5} = 0.339 \pm 0.02$ and for the $\delta = 1$ mm wide nozzle $c_1 = 0.344 \pm 0.02$, which in our opinion differs within the uncertainty of the values. However, from the CFD simulations they obtained somewhat (about 13 – 15%) lower values: $c_{0.5} = 0.29 \pm 0.04$ and $c_1 = 0.3 \pm 0.03$.

1.3 Frequency and phase characteristics of the edge tone

As has been shown, the literature is consequent in the proposition that the oscillation frequency is roughly proportional to the mean exit velocity of the jet and inversely proportional to the k^{th} power of the nozzle-to-wedge distance:

$$f \propto \frac{u}{h^k}. \tag{15}$$

Sometimes an additive constant in one or both of the relationships is also present such as

$$f \propto \frac{u + c_u}{h^k + c_h}.$$

About the value of the exponent k there has been a long debate. In the early phase of the research $k = 1$ was favoured (Brown and other researchers before him [5], Curle [9]) later it became generally accepted that $k = 3/2$ (Curle using Savic's results [9], Holger et al. [10], Crighton [8]). In 1942 Jones [12] found a variety of exponents, all between 1 and 3/2, depending on the stage number. Recent research (Bamberger et al. [2]) and also the results of our experimental and numerical studies indicate that $k = 1$ is more accurate.

In order to ensure comparability, the discussed frequency formulae were transformed to Strouhal numbers and doing so it turned out that all of them can be described in the following form:

$$St\left(Re, \frac{h}{\Delta}\right) \approx \left(c_1 - \frac{c_2}{Re}\right)\left(\frac{1}{h/\delta} - c_3\right) \tag{16}$$

Table 1 shows the values of the coefficients for the first three stages. The experiments of Brown and Jones agree acceptably well (for $h/\delta = 10$ above $Re \approx 150$), the experiments of Brackenridge have a non-negligible but still not too high deviation from these results (above $Re = 200$). The formulae from the theoretical considerations tend to over-estimate the results of the measurements. It can be shown that for low Reynolds numbers and/or low nozzle-to-wedge distances the curves separate and the difference can easily be more than 100%. For higher Reynolds numbers or nozzle-to-wedge distances the differences between the formulae are somewhat smaller but still can reach 25%.

All of the above-mentioned theories can be summarised so that the disturbances on the jet born somewhere near the nozzle, they travel to the wedge, where they somehow interact with it. As a result of this interaction a "signal" is sent to the location of the birth of the disturbances.

As Powell suggests: the oscillating jet creates an oscillating force on the wedge, that creates a dipole sound source. The generated sound then excites the jet – at low Mach numbers with no time delay – and a new disturbance is born that grows as it travels downstream to the wedge.

The phase relation of this loop can be summarised in the following equation:

$$h = \lambda\left(n + \varepsilon\right) \tag{17}$$

where λ is the wavelength of the disturbance, n is a whole number corresponding to the stage number, and ε is a small number indicating that the effective resonance length of the edge tone system somewhat differs from h.

There is no agreement in the literature about the value of ε, it may also depend on the details of the configuration and on the stage number. The most often occurring value is 0.25 (Curle [9], Powell [23]), Holger et al. [10] found values between 0.35 and 0.5 depending on the stage but negative values are also suggested –0.2 (Nonomura et al. [17,18]), –0.25 (Kwon [14,15]) or –3/8(Crighton [8]). One reason for the uncertainty in the dependence of the frequency of oscillation on h is the uncertainty of ε. The exact positions where the dipole source is located (i.e. at the tip of the wedge or at a certain distance away downstream from the tip) and where the sound generated by the acoustic dipole source excites the jet (directly at the nozzle, or somewhat further downstream) are still not explored.

Also the theories presented usually assume that the wavelength and convection velocity of the disturbance do not change

Tab. 1. Parameters of the St (Re; h/δ) relationships (equation (16)) by different authors

Stage	Author	c_1	c_2	c_3	k
Stage I	Brown [5]	0.4659	12.06	0.007	1
	Jones [12]	0.39	0	0	1
	Curle [9]	0.625	0	0.0267	1
	Curle-Savic [9]	1.43	0	0	3/2
	Brackenridge [3]	0.6298	38.4	0.0235	1
	Holger [10]	1.532	0	0	3/2
	Crighton [8]	2.477	0	0	3/2
	Kwon [15] (with $Ma \approx 0$)	0.45	0	0	1
	Bamberger et al. [2] (exp.)	0.513	0	0	1
	Bamberger et al. [2] (CFD)	0.443	0	0	1
Stage II	Brown	1.072	27.74	0.007	1
	Jones	1.217	0	0	1.14
	Curle	1.125	0	0.0148	1
	Curle-Savic	3.46	0	0	3/2
	Brackenridge	1.512	92.2	0.0235	1
	Holger	3.332	0	0	3/2
	Crighton	10.385	0	0	3/2
	Kwon (with Ma ≈ 0)	1.05	0	0	1
Stage III	Brown	1.77	45.83	0.007	1
	Jones	2.52	0	0	1.22
	Curle	1.625	0	0.0103	1
	Curle-Savic	6	0	0	3/2
	Holger	6.057	0	0	3/2
	Crighton	21.32	0	0	3/2
	Brackenridge	2.645	161.3	0.0235	1
	Kwon (with Ma ≈ 0)	1.65	0	0	1

between the nozzle and the wedge, and thus the phase of the disturbance decreases linearly in proportion to the distance but this was found not to be true (Stegen and Karamcheti [25], second part of this publication).

Neglecting these "minor" problems, assuming that the disturbance has to travel the nozzle–wedge distance (Stage I with $\varepsilon = 0$, thus $\lambda = h$) with the mean speed of disturbance propagation that is about 40% of the mean exit velocity ofjet (second part of this publication), the period of one feedback loop is about

$$T \approx \frac{h}{0.4 \cdot u}$$

and so the frequency of the first stage oscillation would be about

$$f \approx \frac{0.4 \cdot u}{h},$$

which is very close to the above formula of Jones for the first stage. For the higher stages this heuristic model does not work.

The flow field of the edge tone was investigated both by numerical and experimental means. Section 2 briefly describes the Computational Fluid Dynamics (CFD) and the experimental setups, the qualitative results obtained by the two methods are discussed in Section 3 and the quantitative discussion of the results is presented in the second part of this publication. At last at the end of the second part a hypothesis that should be further investigated is presented: the Strouhal number of the edge tone is determined rather by the energy flux than by the mass flow rate of the jet.

2 The CFD and experimental setups

2.1 The CFD setup

ANSYS-CFX (Releases from CFX-5.7.1 to ANSYS-CFX v14; product of ANSYS Inc. Southpointe 275 Technology Drive Canonsburg, PA 15317, f1]) was used to simulate the flow. This solver is based on a finite volume scheme, and uses an iterative method to solve the Navier-Stokes equations. In our case the iteration targets are the conservation of mass and momentum.

The flow was assumed to be two-dimensional (2D). Although the software is only capable of calculating flows in 3D domains discretised with 3D elements, it is still possible to calculate planar flows. For this, the domain of the planar flow and the

mesh discretising it have to be extruded in the third direction with only one layer of elements. The height of this layer can be chosen arbitrarily. As long as the aspect ratio of the elements is moderate, the magnitude of the extrusion does not affect the result of the simulation. With symmetry boundary conditions prescribed on the bottom and top surfaces of the extruded domain, the simulation leads to a planar flow.

Air at 25°C ($\rho = 1.185\,\mathrm{kg/m^3}, \mu = 1.831 \cdot 10^{-5}\,\mathrm{kg/ms}$) was used as fluid. Because of the moderate Reynolds number and low Mach number regions ($Re = 60 - 2000$, $Ma = 0.003 - 0.09$) the flow was assumed to be laminar – thus no turbulence model was used – and incompressible. Second order accurate spatial ("High resolution" scheme) and temporal ("Second order backward Euler" scheme) discretisations were used. It has been tested to what extent the initial condition influences the result. Simulations with initially quiescent fluid and initially steady state flow have been performed. It turned out that the initial condition has no influence on the final character of the flow. No special measures had to be taken to initiate the oscillation; the oscillation set in spontaneously after a short transient period.

The numerically investigated edge tone configuration had a nozzle width of $\delta = 1$ mm with varying nozzle-to-wedge distances and varying jet velocities. Detailed mesh and time step dependence study was carried out at a fixed configuration ($Re = 200$, $h/\delta = 10$). Also a criterion for the value of the time step was determined in order to keep the numerical error at the constant value of the reference state also in the case of simulations at higher Reynolds numbers. These are all discussed in more detail in a former paper of the authors [21].

A 3D CFD simulation was also carried out at a Reynolds number of 225 to verify the planar nature of the flow. $Re = 225$ was chosen as that was the highest Reynolds number where a pure first stage oscillation was found in the 2D simulations. The width of the nozzle was the same as in the 2D simulations ($\delta = 1$ mm) and the nozzle-to-wedge distance was $h = 10$ mm. The nozzle and the wedge had different heights: 25 mm and 70 mm, respectively. This was done to allow the jet to spread in the z direction and to have the full effect on the wedge while minimizing the end effects. This edge tone setup was placed in a 90 mm x 151 mm x 70 mm rectangular domain. Again a block-structured hexahedral mesh was used (Figure 9 of [27]). In the central region ($-12.5 < z < +12.5$ mm, where $z = 0$ is the middle plane) the elements had a height of 1 mm. From the end of the nozzle in the following 7.5 mm the height of the elements grew up to 3 mm from where the elements had a height of 3 mm. The mesh in any cross section perpendicular to the z direction had the same resolution in the nozzle-wedge region as the mesh used in the 2D simulations and was coarser at the boundaries. The mesh contained about 685 000 elements. Comparison between the results of the 2D and the 3D simulations will be given later in Section 3.1.

2.2 The experimental setup

The experimental rig to produce the edge tone phenomenon is described in detail in a former paper of the authors [26]; here only a short overview will be given.

Shop air with a pressure reduced to bar by a pressure reducing valve was led by 3/4" reinforced flexible plastic tubes to a cylindrical pressure reservoir with a volume of 57 l. A mass flow rate sensor (Sensortechnics, Honeywell AWM700, working on a heated element principle with a voltage output) was built into the line between the pressure reducing valve and the reservoir tank to determine the mean velocity of the jet. There was a long copper pipe section before the sensor to ensure undisturbed inflow. Two different nozzles were used to create a top hat or a parabolic velocity profile for the jet. They will be referenced as the "top hat nozzle" and "parabolic nozzle". The top hat nozzle was formed by two quarter-cylinders ensuring a quick contraction. In the parabolic nozzle two parallel 150 mm long plates with a 15 mm radius rounded entry ensured the development of the parabolic velocity profile. The shape of the cross section of the nozzles was rectangular with an aspect ratio over 20 which ensured good two-dimensionality in the central region. When using the top hat nozzle, visualisation was possible with an incense stick inserted just before the converging part of the nozzle. The smoke filament was illuminated with floodlight and the image was recorded with a high speed digital camera (LaVision ImagerCompact) taking images with a maximum frequency of 90 Hz and a spatial resolution of 320x240 pixels. No visualisation was made in the parabolic case. The wedge was made of well-polished solid steel with an angle of 30°. Its height (z direction) was 150 mm, i.e. this dimension was twice as long as the slit of the nozzle to avoid end effects. The distance between the nozzle and the wedge was adjustable in the range of 5 mm to 53 mm. A pressure transducer (Sensortechnics, 113LP01D-PCB) was built into the wedge to measure the surface pressure at a distance of 26.2 mm from the tip of the wedge. The amplified analogue signal of the pressure transducer was used to determine the frequency of oscillation via FFT.

3 Results

3.1 Verification of the planar nature of the flow

Both the 3D CFD simulation and the experiments verified that the flow is indeed two-dimensional. In the 3D CFD simulation, similarly to the 2D case, after a short transient part during which the edge tone oscillation evolves, a stable first stage oscillation evolved with a frequency of 130 ± 0.5 Hz. The role of the higher harmonics could be neglected. The frequency of oscillation was equal in the 2D and 3D simulations and the structure of the flow was very similar in the two cases.

The streamlines that exit from the nozzle (shown e.g. in Figure 14 of [27]) were parallel between the nozzle and the wedge, and only separated after a short distance from the tip of the wedge. The $z = 0$ mm plane, as well as the streamlines

are coloured by the velocity magnitude. Similar observations were made during the experiments. The flow was visualised with several incense sticks at different heights simultaneously. The trace lines at different heights oscillated together.

3.2 Varying the Reynolds number at a fixed geometric configuration

The dimensionless nozzle-to-wedge distance was set to around $h/\delta \approx 10$, while the Reynolds number of the flow was varied by varying the mass flow rate. Table 2 shows the values of h/δ and the investigated Reynolds number ranges during the CFD simulations and during the experiments in the top hat and the parabolic cases.

3.2.1 Top hat profile

At first measurements and CFD simulations were carried out at very low Reynolds numbers ($Re < 60$), where no edge tone activity was found.

At $Re \approx 60$ in the simulations and also in the experiments an intermittent first stage edge tone oscillation sets in. In the case of the CFD simulations this means that the simulations produce a steady flow field but with a small disturbance (the exit velocity of the jet was increased with a transversal component of 0.5 m/s – that is approximately 50% of the jet mean velocity in the $Re = 60$ case – for about 100-150 steps) the oscillation could be initiated and it remained. In the case of the experiments the edge tone phenomenon was switching on and off, in some cases it could be observed. Above $Re = 100$ a stable first stage edge tone oscillation occurred without any external excitation both in the simulations and in the experiments.

At $Re = 250$ in the simulations and $Re = 200$ in the experiments the second stage of the edge tone appeared next to the first stage. With the advent of the second stage the frequency and thus the Strouhal number of the first stage dropped by about 14.5 ± 2% in the simulations and 14 ± 2% in the experiments compared to the value extrapolated from the pure first stage – using the formula to be introduced in the second part of the publication – to the current inlet velocity. This drop is in good agreement with the results of Jones [12] and of Stegen and Karamcheti [25].

Figure 3 shows the Reynolds number dependence of the Strouhal number of the first stage in the pure and in the multi-stage modes. Solid and dashed curves in the figure show the best fit with formulae to be introduced in the second part of the publication fitted on the observed Strouhal numbers of the first stage in the pure (solid) and multi- (dashed) stage modes. The thick solid line gets thin at the appearance of the second stage from where extrapolated values are used for the graph. Right of this point the drop of the Strouhal number of the first stage – the difference between the thin solid line and the dashed line of the same colour – can be nicely observed. Error bars represent the width of the spectral peak in the case of the simulations, and

Tab. 2. Values of h/δ and Reynolds number ranges for Reynolds number dependence studies

	Top hat		Parabolic	
	CFD	Exp.	CFD	Exp.
h/δ	10	10.26 ± 0.23	10	9.72 ± 0.44
Re	0 – 1800	0 – 1200	0 – 2000	0 – 1400

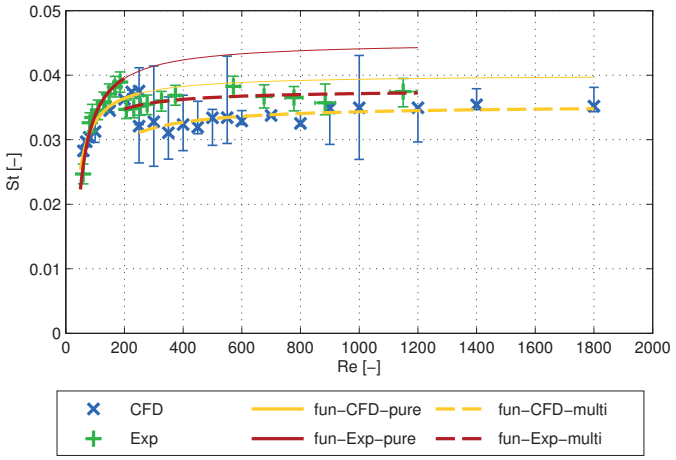

Fig. 3. Reynolds number dependence of the Strouhal number of the first stage; top hat profile, $h/\delta \approx 10$; fun-CFD-pure, fun-CFD-multi, fun-Exp-pure and fun-Exp-multi are the functions described by Equation (2) and Table 1 of the second part of this publication in the case of CFD simulations (yellow lines) or experiments (red lines) and pure (solid lines) or multi-stage modes (dashed lines)

the uncertainty of the measurements in the case of the experiments. The difference between the red (experimental) and the yellow (CFD) curves is usually around 7.5 – 8.5% and only grows over 10% at the appearance of the first stage – when the steepness of the curves are quite high, thus a small error in the Reynolds number results in a large error in the Strouhal number – or at the appearance of the second stage. The magnitude of the difference is within the range of the uncertainty of the Strouhal number determination. The first stage was always present parallel to the second stage, the question was only if the second stage is dominant or their strengths are comparable. For example Figure 4 shows two parts of the same CFD simulation ($Re = 600$, $h/\delta = 10$, top hat jet profile). Above is a short part of the time history of the force acting on the wedge and below is the corresponding spectrum of a somewhat longer part of the signal. First the two stages were comparable (left side) then later the second stage became dominant (right side).

Brown [5] found the second stage to set in around $Re = 220$. He also mentioned to observe simultaneous existence of stages. He took photos of the oscillating flow illuminated by light through a stroboscopic disk. Therefore – except for some special cases – Brown was only able to measure the frequency of

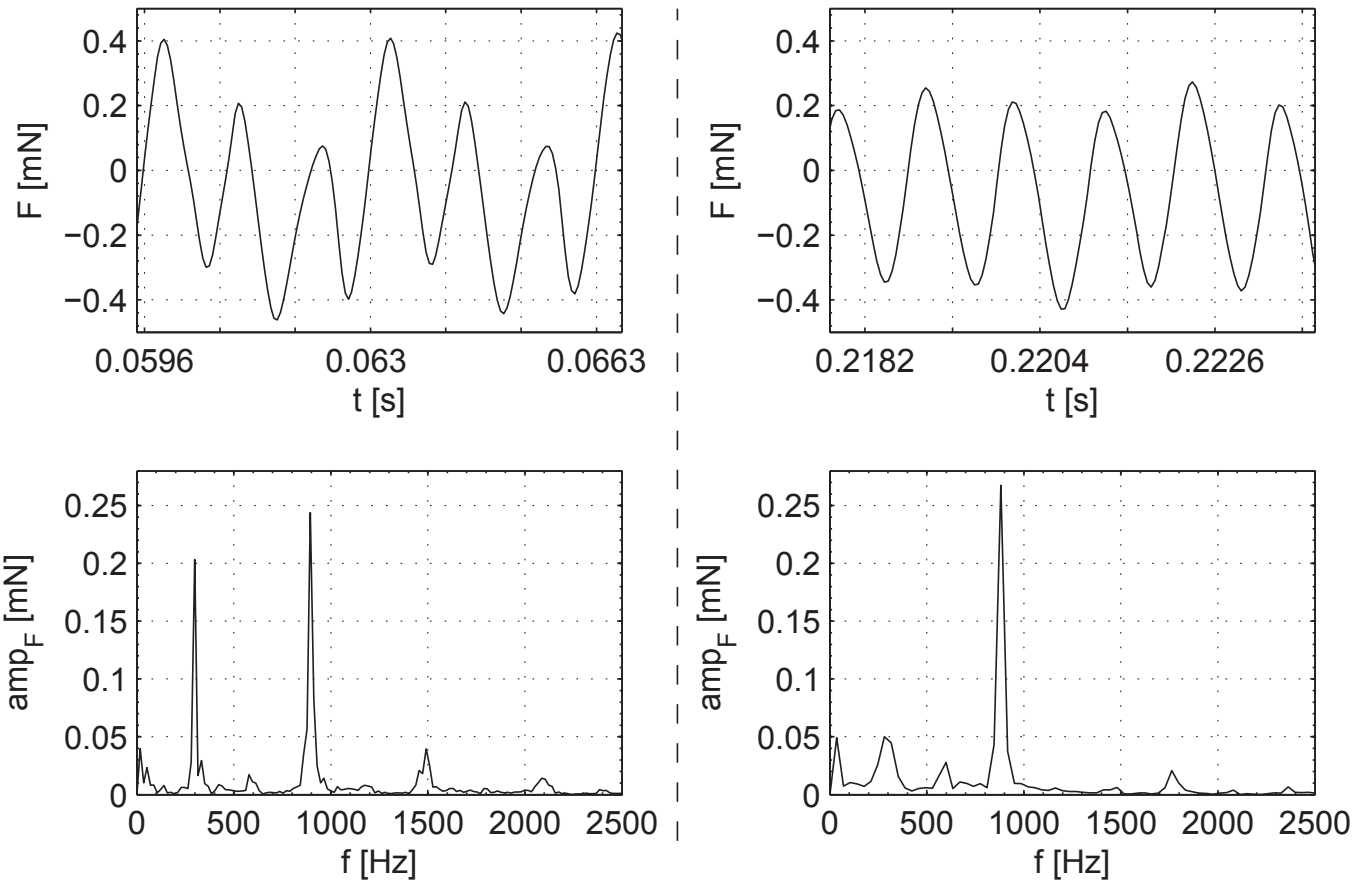

Fig. 4. Stage I & II coexistence edge tone oscillation in the CFD simulations at $Re = 600$, $h/\delta = 10$ with top hat jet profile. The two sides represents two parts of the same force signal: left side: the first and the second stages are comparable; right side: the second stage dominates

the dominant stage when several stages coexisted. From these special cases he concludes that the frequency of the first stage, when coexisting with other stages is about 7% lower than using the formula deduced from the frequencies of pure first stage oscillations. Brown states that his formula in some cases may have an error of 6%, thus he concludes that the frequency of the first stage remains practically unaltered, although it could mean also that the drop is even higher than 7% which would agree with the results of Jones [12] and also with our computational and experimental results.

With the advent of the third stage the first two stages remained, thus three stages coexisted superposed on each other. In the CFD simulations the third stage first appeared in the $Re = 900$ simulation but it was not yet stable, the third stage was observable only during a short period of the whole simulation. From $Re = 1400$ the third stage was present in the whole simulation. In the experiments the third stage appears surprisingly early, at around $Re \approx 250$. This was only discoverable when using the pressure sensor for frequency measurement because when the third stage sets in, at first it is very weak, and from the three stages that are superposed only the dominant second one can be seen by flow visualisation. Figure 5 shows photos taken of the oscillating flow at around $Re = 400$ and 700 respectively, and the spectrum of the corresponding pressure signals. Three half waves can be observed in the $Re = 700$ case, and only two half waves in the $Re = 400$ case but the spectral peak for the third stage is present in both spectra. Figure 5 shows a typical nonlinear effect too: often when two or more stages coexist, peaks appear in the spectra at the difference or at the sum of the frequencies of these stages. At $Re \approx 400$ in the spectrum of the output signal of the pressure transducer a peak at the difference of the frequencies of the second and the first stages ($f_2 - f_1$) can be observed. This was observed experimentally by Brackenridge and Nyborg [4] and also by Lucas and Rockwell [16].

3.2.2 Parabolic profile

When changing the mean exit velocity of the jet, the parabolic profile jet-edge configuration shows a remarkably different behaviour from the top hat jet-edge configuration. At the beginning – at low Reynolds numbers – similar behaviour can be observed: after reaching a lower Reynolds number limit ($Re = 50$ in the CFD simulations and $Re \approx 85$ in the experiments) the first stage edge tone oscillation sets in.

As the Reynolds number is increased, the second stage appears together with the first stage at $Re = 150$ in the simulations and $Re \approx 180$ in the experiments, both of them coexisting.

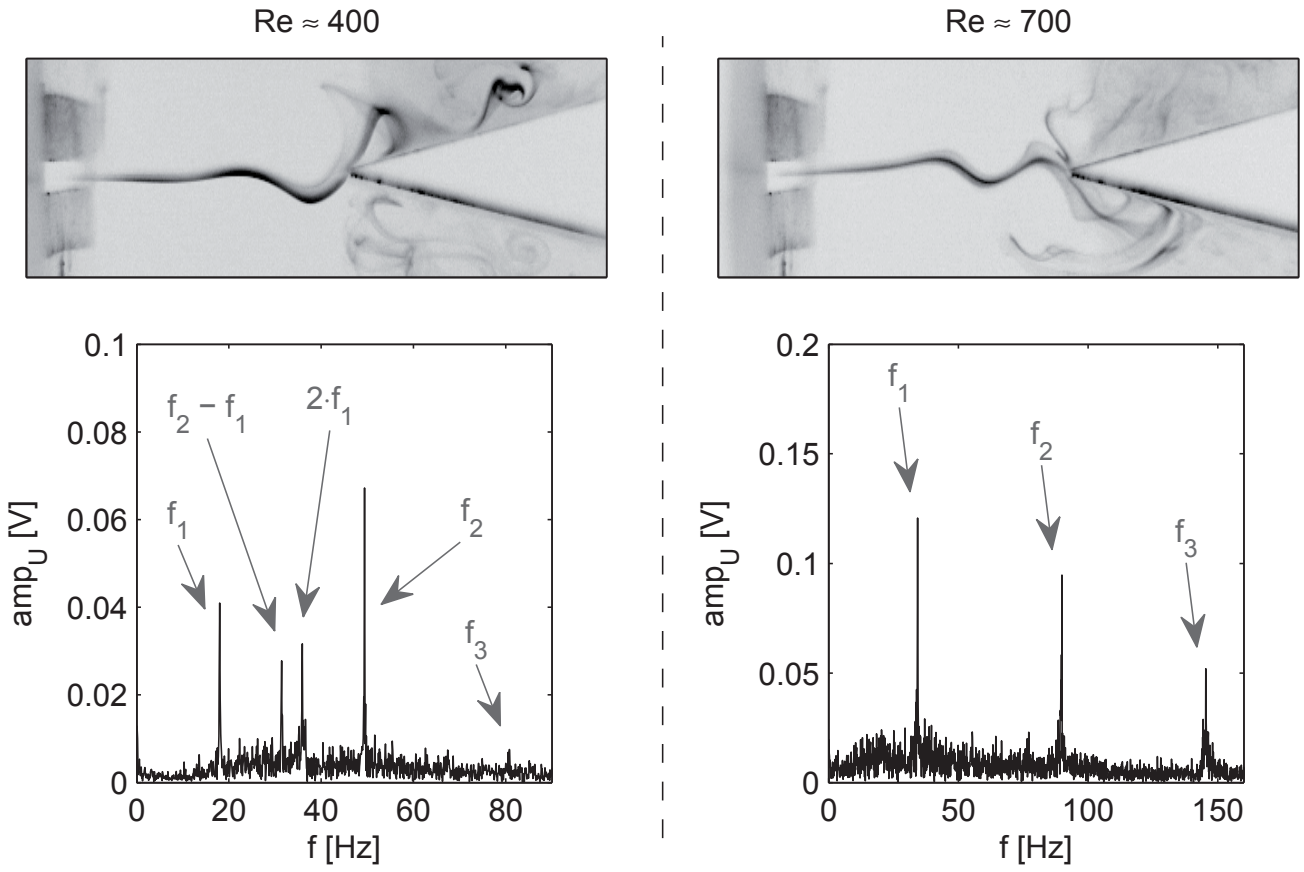

Fig. 5. Stage III edge tone oscillation in the experiments: left side: $Re \approx 400$; right side: $Re \approx 700$; upper line: photo taken of the visualised flow; bottom line: the spectrum of the output signal of the pressure transducer; f_n is the frequency of the n^{th} stage, $n = 1, 2$ or 3

As in the top hat case, the frequency of the first stage drops. In this case the magnitude of the drop is about $9.7 \pm 2.2\%$ that is somewhat smaller compared to that in the top hat case. This drop is only observable from the results of the experiments as in the CFD simulations the first stage disappeared soon after the onset of the second stage, and thus there were not enough data for the frequency of the first stage from multi stage operation mode to reliably detect the frequency drop. Further increasing the Reynolds number, a qualitatively different behaviour from the top hat case can be observed: from $Re = 300$ in the CFD simulations and $Re \approx 360$-420 in the experiments the first stage disappears and a pure second stage oscillation can be found. This is the highest stage found with the help of CFD simulations.

With increasing Reynolds number in the experiments (at $Re \approx 650$) the second stage disappears and the third stage of the edge tone comes into being but at the same time the first stage reappears, both coexisting. At the highest Reynolds numbers a pure third stage oscillation was observed (from $Re \approx 900$).

Similar behaviour can be observed when decreasing the Reynolds number but having stage jumps at different Reynolds numbers, and without a pure second stage oscillation. It was found that in the Reynolds number 350-600 region when increasing the Reynolds number there is a pure second stage oscillation (the first stage disappeared) but when decreasing the Reynolds number (coming from a third stage oscillation superposed on the first stage) the coexistence of the third and the first stages lasts longer, and there is no pure second stage oscillation at all. This hysteretic effect and also more about the stage jumps are discussed in detail in [26].

3.2.3 Comparison: top hat vs. parabolic velocity profile

The following differences in the behaviour of the two cases have been found:

- In the parabolic case the first and the second stages appear at around the same Reynolds number as in the top hat profile case but in the CFD simulations no third stage was found at all and in the experiments it appears only at a much higher Reynolds number: the third stage comes into being at $Re \approx 600$ in the parabolic case and at $Re \approx 250$ in the top hat case.
- In the case of the top hat profile, when the Reynolds number is increased and a new stage appears, the old, lower stage exists further and in most of the cases the two or three stages are superposed on each other. Since the stage frequencies are not harmonically related to each other, the ensuing motion is strictly speaking not periodic. There is no sign at higher Reynolds numbers that the lower stage would tend to disappear. Contrary to this,

in the parabolic case the lower stages disappear when a higher stage appears thus pure second and pure third stage oscillations can also be found.

- In the parabolic case – both in the experiments and in the CFD simulations – almost everywhere strong frequency component at one-third of the fundamental and also at of its multiples can be detected. This finding agrees strikingly with the experimental findings of Lucas and Rockwell [16] and Kaykayoglu and Rockwell [13] who reported exactly the same.
- For the parabolic profile the frequency of the oscillation (and thus the Strouhal number) is about 15-20% larger relative to the top-hat profile. Ségoufin et al. [7] found experimentally that the top hat profile produces about 50% higher frequencies than the parabolic profile with the same *maximum* velocity. Comparing their results of top hat and parabolic edge tones at equivalent Reynolds numbers (based on the mean velocity) it turns out that in their measurements the frequency of oscillation is almost equal at lower Reynolds numbers (when the oscillation sets in) but increases faster in the parabolic case resulting in 10-20% higher frequencies – apart from the low Reynolds number case – that is consistent with our results.
- In the parabolic case the rms value of the pressure fluctuations rose about 35% relative to the top-hat profile case.
- With a constant pressure and zero velocity initial condition the initial transient (the time until the steady state oscillation is reached) was about half as long for the parabolic as for the top hat case. This was only investigated with CFD.
- Some of these findings (but not all) can be tentatively explained by the fact that about 20% more momentum and about 54% more energy is injected into the system in the case of a parabolic profile for the same Reynolds number than in the top hat profile case.

3.3 Varying the nozzle-to-wedge distance

The Reynolds number was kept constant while the nozzle-to-wedge distance was varied. Exact values and intervals of the parameters can be found in Table 3. In all cases qualitatively the same behaviour could be observed. The boundaries of the stages are a bit different for different Reynolds numbers and in the parabolic case higher stages can be present alone just like it was found in the Reynolds number dependence study.

In the top hat case the following behaviour was observed (Figure 6)

- The first stage appears at around $h/\delta \approx$ 3-4 (lower values at higher Reynolds numbers).
- At around $h/\delta \approx$ 7-11 the second stage appears together with the first stage and at the same time a slight drop in the trend of the Strouhal number of the first stage can be observed.

Tab. 3. Values of the Reynolds numbers and and ranges of h/δ values during the h/δ value dependence studies

	Top hat		Parabolic
	CFD	Exp.	Exp.
Re	350	≈189, 326 and 380	≈192, 348, 586 and 911
h/δ	0 - 15	0 - 16	0 - 17

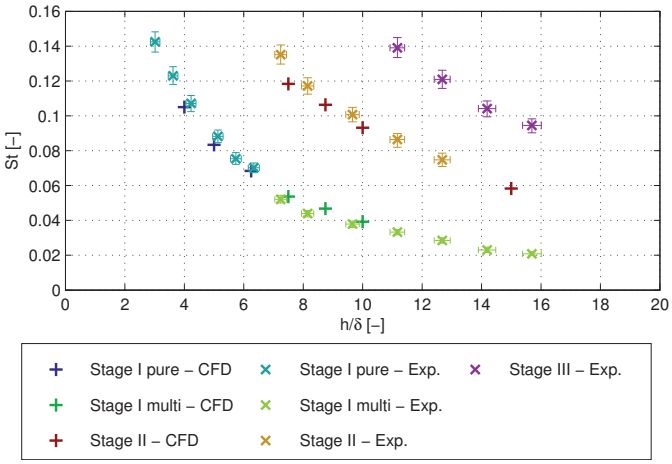

Fig. 6. Dependence of the Strouhal number on the dimensionless nozzle-to-wedge distance; top hat profile, $Re = 350$ and $Re \approx 380$ for the CFD and experimental results, respectively

- In the experiments for the higher Reynolds numbers ($Re \approx$ 326 and 380) as the distance is increased at $h/\delta \approx$ 11-13 the third stage appears parallel to the first and the second stages.
- With increasing h/δ value the second stage disappears and the first and third stage coexist.

Figure 6 shows the Strouhal numbers from the experiments at $Re \approx 380$ and from the CFD simulations at $Re = 350$. The agreement is excellent, especially considering that the Strouhal number at a fixed h/δ value still grows a bit in the $Re = 350$-380 region. The experiments at the other two Reynolds numbers result in quite the same trend.

In the parabolic case – where only experimental investigations were carried out – several kinds of stage constellations can be observed:

- The first stage sets in at around the same h/δ value as in the top hat case ($h/\delta \approx$ 4-5, lower values at higher Reynolds numbers).
- At around $h/\delta \approx$ 6-10 the second stage appears next to the first stage and at the same time a slight drop of the trend of the Strouhal number of the first stage can be observed.
- Increasing the distance between the nozzle and the wedge sometimes but not always a pure second stage oscillation can be found.
- At the onset of the third stage (at around $h/\delta \approx$ 9-17) first it

coexists with the first and the second stages, then later the second stage disappears and the first and third stages remain.

- Further increasing the value of h/δ a pure third stage oscillation can be observed.
- For the highest distances and Reynolds numbers combination (at $h/\delta \approx$ 15-17 and $Re \approx$ 570 and 890) the fourth stage also appeared alone or coexisting with the third stage.

The presence of hysteresis was investigated in the parabolic case at $Re \approx 380$. No hysteresis was found; the stage jump occurred at the same wedge position when increasing and when decreasing the distance between the nozzle and the wedge.

References

1 **ANSYS Inc.**, Southpointe 275 Technology Drive Canonsburg, Pennsylvania 15317. ANSYS-CFX. http://www.ansys.com/Products/Simulation+Technology/Fluid+Dynamics/Fluid+Dynamics+Products/ANSYS+CFX. (last visited Jan 6, 2014).

2 **Bamberger A., Bänsch E., Siebert K. G.**, *Experimental and numerical investigation of edge tones*. Journal of Applied Mathematics and Mechanics, 84(9), 632-646 (2004). DOI: 10.1002/zamm.200310122

3 **Brackenridge J. B.**, *Transverse Oscillations of a Liquid Jet. I*. The Journal of the Acoustical Society of America, 32(10), 1237-1242 (1960). DOI: 10.1121/1.1907888

4 **Brackenridge J. B., Nyborg W. L.**, *Acoustical characteristics of oscillating jet-edge systems in water*. The Journal of the Acoustical Society of America, 29(4), 459-463 (1957). DOI: 10.1121/1.1908928

5 **Brown G. B.**, *The vortex motion causing edge tones*. Proceedings of the Physical Society of London, 49(5), 493-507 (1937). DOI: 10.1088/0959-5309/49/5/306

6 **Brown G. B.**, *The mechanism of edge-tone production*. Proceedings of the Physical Society, 49(5), 508-521 (1937). DOI: 10.1088/0959-5309/49/5/307

7 **Fabre B., Ségoufin C., de Lacombe L.**, *Experimental investigation of the flue channel geometry influence on edge-tone oscillations*. Acta Acustica united with Acustica, 90(5), 966-975 (2004).

8 **Crighton D.**, *The jet edgetone feedback cycle; linear theory for the operating stages*. Journal of Fluid Mechanics, 234, 361-391 (1992). DOI: 10.1017/S002211209200082X

9 **Curle N.**, *The mechanics of edge-tones*. Proceedings of the Royal Society A, 216(1126), 412-424 (1953). DOI: 10.1098/rspa.1953.0030

10 **Holger D. K., Wilson T. A., Beavers G. S.**, *Fluid mechanics of the edgetone*. The Journal of the Acoustical Society of America, 62(5), 1116-1128 (1977). DOI: 10.1121/1.381645

11 **Holger D. K., Wilson T. A., Beavers G. S.**, *The amplitude of edgetone sound*. The Journal of the Acoustical Society of America, 67(5), 1507-1511 (1980). DOI: 10.1121/1.384313

12 **Jones A. T.**, *Edge Tones*. The Journal of the Acoustical Society of America, 14(2), 131-139 (1942). DOI: 10.1121/1.1916209

13 **Kaykayoglu R., Rockwell D.**, *Unstable jet-edge interaction. Part 2: Multiple frequency pressure fields*. Journal of Fluid Mechanics, 169, 151-172 (1986). DOI: 10.1017/S0022112086000575

14 **Kwon Y.-P.**, *Phase-locking condition in the feedback loop of low-speed edgetones*. The Journal of the Acoustical Society of America, 100(5), 3028-3032 (1996). DOI: 10.1121/1.417114

15 **Kwon Y.-P.**, *Feedback mechanism of low-speed edgetones*. The Journal of the Acoustical Society of America, 104(4), 2084-2089 (1998). DOI: 10.1121/1.423722

16 **Lucas M. Rockwell D.**, *Self-excited jet: upstream modulation and multiple frequencies*. Journal of Fluid Mechanics, 147, 333-352 (1984). DOI: 10.1017/S0022112084002111

17 **Nonomura T., Muranaka H., Fujii K.**, *Computational Analysis of Mach Number Effects on Edgetone*. in 'Proceedings 36th AIAA Fluid Dynamics Conference and Exhibit. San Francisco, California', Vol.1, 139-152, AIAA 2006-2876 (2006). Chapter DOI: 10.2514/6.2006-2876

18 **Nonomura T., Muranaka H., Fujii K.**, *Computational Analysis of Mach Number Effects on the Edgetone Phenomenon*. AIAA Journal, 48(6), 1248-1251 (2010). DOI: 10.2514/1.44849

19 **Nyborg W. L.**, *Self-Maintained Oscillations of the Jet in a Jet-Edge System. I*. The Journal of the Acoustical Society of America, 26(2), 174-182 (1954). DOI: 10.1121/1.1907304

20 **Nyborg W. L., Burkhard M. D., Schilling H. K.**, *Acoustical characteristics of jet-edge and jet-edge-resonator systems*. The Journal of the Acoustical Society of America, 24(3), 293-304 (1952). DOI: 10.1121/1.1906894

21 **Paál G., Vaik I.**, *Unsteady phenomena in the edge tone*. International Journal of Heat and Fluid Flow, 28(4), 575-586 (2007). DOI: 10.1016/j.ijheatfluidflow.2007.04.011

22 **Powell A.**, *On edge tones and associated phenomena*. Acustica, 3, 233-243 (1953).

23 **Powell A.**, *On the Edgetone*. The Journal of the Acoustical Society of America, 33(4), 395-409 (1961). DOI: 10.1121/1.1908677

24 **Savic P.**, *On acoustically effective vortex motion in gaseous jets*. Philosophical Magasine, Series 7, 32(212), 245-252 (1941). DOI: 10.1080/14786444108520791

25 **Stegen G. R., Karamcheti K.**, *Multiple tone operation of edgetones*. Journal of Sound and Vibration, 12(3), 281-284 (1970). DOI: 10.1016/0022-460X(70)90072-6

26 **Vaik I., Paál G.**, *Mode switching and hysteresis in the edge tone*. Journal of Physics: Conference Series, 268(1), no. 012031, 11 pages (2011). DOI: 10.1088/1742-6596/268/1/012031

27 **Vaik I., Paál G., Kaltenbacher M., Triebenbacher S., Becker S., Shevchenko I.**, *Aeroacoustics of the edge tone: 2D-3D coupling between CFD and CAA*. Acta Acustica united with Acustica, 99(2), 245-259 (2013). DOI: 10.3813/AAA.918607